

**Table I.** Rate and Equilibrium Constants for Binding Chloride Ion by Hosts **1**<sup>a</sup>

host	temp (°C)	$k_r$ (s <sup>-1</sup> )	$k_f$ (M <sup>-1</sup> s <sup>-1</sup> ) <sup>b</sup>	$K_{eq}$ (M <sup>-1</sup> )
<b>1b</b> <sup>c</sup>	-50	$(2.0 \pm 0.8) \times 10^2$	$(9 \pm 4) \times 10^3$	4 <sub>5</sub>
	-40	$(3.6 \pm 0.4) \times 10^2$	$(2 \pm 1) \times 10^4$	5 <sub>6</sub>
	-30	$(8.4 \pm 0.8) \times 10^2$	$(3.7 \pm 0.8) \times 10^4$	4 <sub>4</sub>
	-20	$(2.0 \pm 0.3) \times 10^3$	$(7 \pm 2) \times 10^4$	3 <sub>5</sub>
	-10	$4 \times 10^3$	$1 \times 10^5$	2 <sub>5</sub>
<b>1c</b>	-20	$3 \times 10^4$	$1 \times 10^6$	3 <sub>3</sub>
<b>1d</b>	-50	$6 \times 10^4$	$3 \times 10^5$	5
	-20	$3 \times 10^5$	$2 \times 10^6$	7
	20	$3 \times 10^6$	$1 \times 10^7$	3

<sup>a</sup>Results from line shape analyses of spectra of CDCl<sub>3</sub> solutions containing hosts and tetrahexylammonium chloride. Error limits, when given, are 1σ for multiple determinations and do not contain an estimate of systematic errors. Single determination values are given without error limits; these values are believed to be accurate to better than ±25% for  $k_r$  and ±50% for  $k_f$ . <sup>b</sup> $k_f$  was calculated from the  $k_r'$  of the simulation and the concentration of free chloride. <sup>c</sup>Averages of four values for -50 to -30 °C and three values for -20 °C.

of the slower exchanging C-8 host **1b** (with 0.5 equiv of Cl<sup>-</sup>) contained two sharp signals at -50 °C that broadened on warming (Figure 1).



The binding of chloride by **1b-d** is described by the simple model in eq 1. Line shape analyses of the spectra containing hosts **1b-d** and chloride gave kinetic results,<sup>9</sup> some of which are listed in Table I. The rates of complexation and decomplexation were slowed appreciably as the chain length decreased; we presume that this reflects steric interactions as the chloride squeezes between two chains to enter or exit the cavities. For host **1b**, studies of solutions of varying concentration indicated that decomplexation ( $k_r$ ) was unaffected by concentration; an Arrhenius treatment for this first-order decomplexation of chloride from the (**1b**·Cl)<sup>-</sup> complex gave an  $E_a$  of  $9.1 \pm 0.5$  kcal/mol (two solutions, 15 measurements between -50 and -20 °C, the error limit is 1σ). The binding constants of hosts **1b** and **1c** at -20 °C were substantially greater than that for host **1d**; apparently the best cavity size for chloride occurs between hosts **1b** and **1c**.

A more dramatic demonstration of size selectivity was found when the C-6 bicycle **1a** was studied. At room temperature the <sup>119</sup>Sn NMR spectrum of **1a** (+148 ppm) was unaltered by the addition of excess chloride. The absence of line broadening or a second signal in the +30 to +40 ppm region in the spectra of **1a** showed that no complexation occurred to the limit of our detection capabilities. With the conservative estimate that even in the most difficult to detect case (slow exchange limit) we would have observed 5% complex if it was present, we can set a limit on  $K_{eq}$  for **1a** of <1 M<sup>-1</sup>. Host **1a** is not Lewis acidic toward chloride!

We have shown that highly selective anion binding in organic solvents is possible with appropriately constructed Lewis acidic hosts even when only two binding sites are available. The selectivity can result from either the exclusion of the guest from an under-sized cavity or the poor fit of the guest within an over-sized cavity. The replacement of chloride on bicycles **1** with a nonlabile electron-withdrawing group should be expected to give hosts that complex a variety of anionic and neutral basic guests selectively.

**Acknowledgment.** This work was supported by the Office of Naval Research.

(9) A two-site exchange model was used.<sup>10</sup> The  $T_2$  values used in simulations were determined experimentally (Varian's CPMGT2 sequence) for host **1b** at 149.2 MHz (0.05 s for the uncomplexed and 0.003 s for the complexed signal).

(10) Sandström, J. *Dynamic NMR Spectroscopy*; Academic: London, 1982.

## Assignment of <sup>15</sup>N NMR Signals in Bovine Pancreatic Trypsin Inhibitor

John Glushka and David Cowburn\*

The Rockefeller University  
New York, New York 10021

Received June 26, 1987

With the development of <sup>1</sup>H detected heteronuclear chemical shift correlation spectroscopy, the detection of <sup>15</sup>N spectra has become possible for peptides and small proteins at natural abundance.<sup>1,2</sup> Recently, reports have shown that <sup>1</sup>H[<sup>15</sup>N] correlation is feasible in small proteins,<sup>3-5</sup> though assignments were incomplete. The analysis of nitrogen chemical shifts of backbone and side chain amides for structural information<sup>6,7</sup> requires more extensive and accurate assignments. In addition, there has recently been considerable interest in studying <sup>15</sup>N enriched proteins,<sup>8-10</sup> and further improvements in understanding the origin of the variation of chemical shifts with primary, secondary, and tertiary structure are likely to be of general use. We have attempted a complete assignment of the <sup>1</sup>H[<sup>15</sup>N] spectra from bovine pancreatic trypsin inhibitor (BPTI), a small (MW 6500) rigid protein which has been the molecule of choice for extensive proton NMR studies.<sup>11,12</sup> The chemical shifts of the backbone amides were then compared to model values, and the resulting differences analyzed with respect to amide hydrogen bonding, to torsional angles, and to other structural features available from the crystal structure and proton NMR studies. The general features of the X-ray crystal structure<sup>13</sup> are thought to be maintained in solution under a variety of temperatures and pH values.<sup>14</sup>

The assignments were derived first with data collected at 68 °C.<sup>15</sup> A phase-sensitive double-quantum-filtered COSY spectrum<sup>16</sup> at this temperature clarified regions of proton overlap and minor differences in proton chemical shifts from published values. A few peptide amide resonances and most carboxamide side chain resonances were not observed due to rapid proton exchange at 68 °C. Ambiguities arising from weak or absent signals and proton

- (1) Bax, A.; Griffey, R. H.; Hawkins, B. L. *J. Magn. Reson.* **1983**, *55*, 301.
- (2) Live, D. H.; Davis, D. G.; Agosta, W. C.; Cowburn, D. *J. Am. Chem. Soc.* **1984**, *106*, 6104-6105.
- (3) Ortiz-Polo, G.; Krishnamoorthi, R.; Markley, J. L.; Live, D. H.; Davis, D. G.; Cowburn, D. *J. Magn. Reson.* **1986**, *68*, 303-310.
- (4) Wagner, G. 27th ENC, Baltimore, MD, 1986.
- (5) Sklenar, V.; Bax, A. *J. Mag. Reson.* **1987**, *71*, 379-383.
- (6) Levy, G. C.; Lichter, R. L. In *Nitrogen-15 NMR Spectroscopy*, Wiley-Interscience: New York, 1979.
- (7) Witanowski, M.; Stefaniak, L.; Webb, G. A. *Annu. Rep. NMR Spectrosc.* **1986**, *18*, 1-761.
- (8) LeMaster, D. M.; Richards, F. M. *Biochemistry* **1985**, *24*, 7263-7268.
- (9) Griffey, R. H.; Redfield, A. G.; Loomis, R. E.; Dahlquist, F. W. *Biochemistry* **1985**, *24*, 817-822.
- (10) Schiksnis, R. A.; Bogusky, M. J.; Tsang, P.; Opella, S. J. *Biochemistry* **1987**, *26*, 2373-2382.
- (11) Pardi, A.; Wagner, G.; Wüthrich, K. *Eur. J. Biochem.* **1983**, *138*, 445-454, and reference therein.
- (12) Wagner, G.; Wüthrich, K. *J. Mol. Biol.* **1982**, *155*, 347-366.
- (13) Deisenhofer, J.; Steigemann, W. *Acta Crystallogr., Ser. B: Struct. Crystallogr. Cryst. Chem.* **1975**, *B31*, 238-250. Wlodawer, A.; Walter, J.; Huber, R.; Sjölin, L. *J. Mol. Biol.* **1984**, *180*, 301-329.
- (14) Wagner, G.; Braun, W.; Havel, T. F.; Schammann, T.; Gö, N.; Wüthrich, K. *J. Mol. Biol.* **1987**, *196*, 611-639.
- (15) As was discussed in a recent paper (ref 5), the experiment of choice for <sup>15</sup>N in water omits the refocusing 180° <sup>1</sup>H pulse but includes hetero-decoupling during acquisition. The authors collected multiquantum <sup>1</sup>H decoupled correlated data in separate blocks, processed them separately, and added the resulting spectra. Though these procedures considerably improve signal-to-noise under favorable conditions, resolution and information can be lost. In the data analyzed here, the limiting factors were the proton spectral overlap and the wide range in intensity of the nitrogen signals. Therefore, we collected only multiquantum coupled data and analyzed the spectra separately. The pattern of doublets with both <sup>1</sup>J(<sup>15</sup>N-<sup>1</sup>H) and <sup>3</sup>J(<sup>1</sup>H-<sup>1</sup>H) allowed differentiation between true signals and noise and thus compensated for the apparent increase in complexity.
- (16) Rance, M.; Sørensen, O. W.; Bodenhausen, G.; Wagner, G.; Ernst, R. R.; Wüthrich, K. *Biochem. Biophys. Res. Commun.* **1983**, *117*, 479-485.

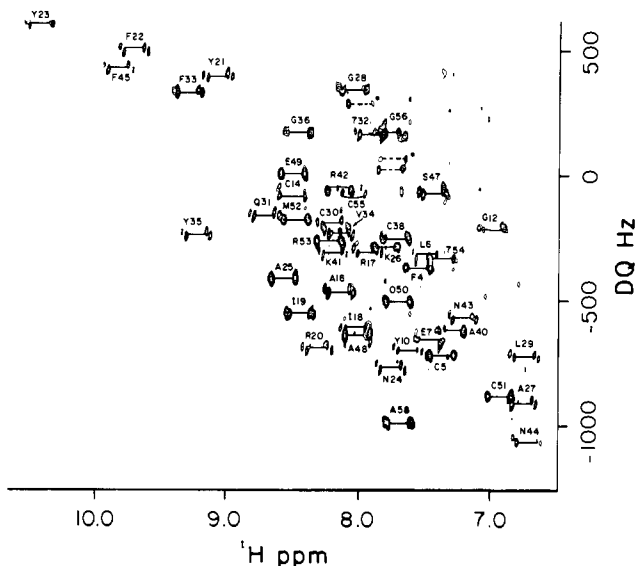


**Figure 1.** Absolute value  $^1\text{H}\{^{15}\text{N}\}$  heteronuclear double quantum spectrum of BPTI in 10%  $\text{D}_2\text{O}/90\%$   $\text{H}_2\text{O}$ , pH 4.6, 23 mmol, at 68 °C. The pulse sequence<sup>1</sup> used was  $\Theta_x^\circ(^1\text{H})-\tau-90_\phi^\circ(^{15}\text{N})-t_1-90_x^\circ(^{15}\text{N})$ -Acquire $_\phi^\circ(^1\text{H})$ , where  $\Theta$  was generally a Redfield 214 selective pulse<sup>25</sup> and  $\tau = 1/2J$ . The proton carrier frequency was at 8.77 ppm relative to internal trisilylpropionic acid reference. The data matrix was  $4096 \times 128$  with acquisition times of 680 and 16 ms for  $t_2$  and  $t_1$ , respectively. For each  $t_1$  block, 1200 accumulations were taken, with an interacquisition delay of 100 ms for a total accumulation time of 33 h. The data were processed with a Gaussian function applied to  $t_2$  and zero filling to 512 points in  $t_1$ . Doublets split by  $^1J_{\text{NH}}$  couplings are joined with a line and labeled with their assignment. Peaks labeled with a star are thought to belong to slowly exchanging Asn 43 and 44 carboxamides. Missing from this plot are signals from D3, K15, G37, R39, K46, and G57. D3, R39, and K46 were observed at other temperatures; K15, G37, and G57 remain unassigned.

overlap were overcome by collecting data under different conditions. At 50 °C and pH 3.5, additional amides and some carboxamide  $^{15}\text{N}$  signals were visible, and the proton data available corroborated previous assignments. At 35 °C, pH 4.6, more signals were visible, though the lack of detailed proton data allowed for only partial assignments.

In total 50 of the 53 amides having observable protons were assigned.<sup>17</sup> A complete 2D contour plot of one of the data sets is shown in Figure 1.<sup>18</sup> In accordance with the extensive studies of  $^{13}\text{C}$  and  $^{15}\text{N}$  shifts in similar smaller structures, it is reasonable to expect significant substituent effects for atoms up to four bonds away.<sup>19</sup> These substituent effects can be lumped into a residue substituent effect for the amino acyl residue and a nearest neighbor effect for the previous amino acyl residue. The former can be obtained from values measured by using *N*-acetyl amino acids in DMSO, which presumably reflect primary effect of side chains.<sup>20–22</sup> These values are then adjusted to reflect neighboring

(17) Assignments for C14, E49 and D3 are considered tentative, due to proton overlap, and the absence of signals for D3 at 68°. No assignments were given to K15 and G57 due to absence of peaks at the expected proton resonance at 68°. At lower temperatures, K15 peaks remained ambiguous, and tentative G57 doublets could not be rigorously separated from carboxamide peaks. The amide proton of G37 has been assigned upfield at 4.3 ppm (Tuchsen, E.; Woodward, C. *Biochemistry* **1987**, *26*, 1918–1925), and no signals were observed in this region of the heterocorrelated spectra.

(18) Complete technical details of assignments and their tabulation will be presented in a full article.

(19) In a typical peptide fragment, these atoms will be 1-bond ( $\alpha$ )  $\text{H}'_i$ ,  $\text{C}'_i$ ,  $\text{C}'_{i-1}$ ; 2-bond ( $\beta$ )  $\text{C}'_i$ ,  $\text{C}'_{i-1}$ ,  $\text{C}'_{i-2}$ ,  $\text{C}'_{i+1}$ ; 3-bond ( $\gamma$ )  $\text{C}'_i$  substituents,  $\text{C}'_{i-1}$  substituents,  $\text{N}'_{i+1}$ ,  $\text{N}'_{i-1}$ ; 4-bond ( $\delta$ )  $\text{C}'_i$  substituents,  $\text{C}'_{i-2}$ ,  $\text{H}'_{i-1}$ ,  $\text{C}'_{i+1}$ ,  $\text{H}'_{i+1}$ .

(20) Live, D. H.; Wyssbrod, H. R.; Fischman, A. J.; Agosta, W. C.; Bradley, C. H.; Cowburn, D. *J. Am. Chem. Soc.* **1979**, *101*, 474–479.

(21) Live, D. H.; Davis, D. G.; Agosta, W. C.; Cowburn, D. *J. Am. Chem. Soc.* **1984**, *106*, 1939–1942.

(22) Cowburn, D.; Live, D. H.; Agosta, W. C. In *Proc. Conversation in Biomolecular Stereodynamics*; Sarma, S., Ed.; Adenine Press: Albany, NY, 1981; pp 345–351.

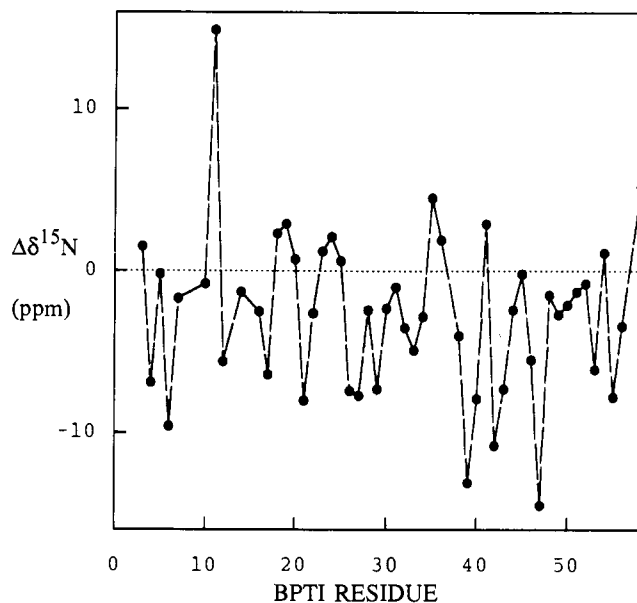


**Figure 2.** Deviations of  $^{15}\text{N}$  chemical shifts,  $\Delta\delta^{15}\text{N}$ , for each residue where  $\Delta\delta^{15}\text{N} = \Delta_{\text{obsd}} - \Delta_{\text{N-acetyl amino acid in DMSO}} - \Delta_{\text{nearest residue correction}} - \Delta_{\text{solvent chang}}$ . Dashed lines connecting points are for visual display purposes only.

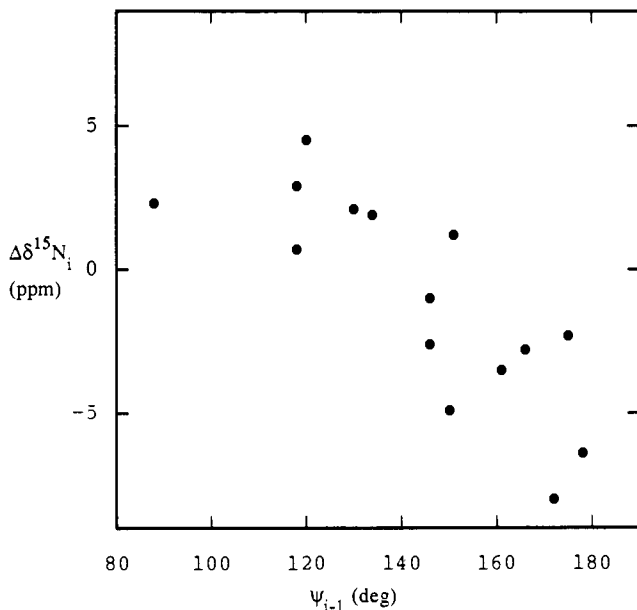


**Figure 3.** Value of the chemical shift deviation,  $\Delta\delta^{15}\text{N}$  (see Figure 2) for  $i$ th residue amides found in  $\beta$  sheets, plotted against the  $\psi$  angle for the preceding residue.

group effects and the solvent change from DMSO to water.<sup>23</sup> The differences between the backbone amide nitrogen shifts and the “corrected” shifts of the model compounds should then reflect the effects of secondary and tertiary structural features. Though these estimates of the shifts arising from the primary structure, and therefore the calculated chemical shift deviations arising from secondary structure, are approximate, a semiquantitative analysis is still possible. The degree of chemical shift deviation can be seen for individual residues in Figure 2. There is a much greater deviation than is observed in smaller peptides, e.g., oxytocin.<sup>20</sup>

Work done on small peptides and polypeptides has shown that changes in solvent and hydrogen bonding have profound effects on nitrogen chemical shifts, and so similar expectations might be had for BPTI.<sup>7</sup> Amides that are buried or exposed to solvent or are involved in varying degrees of hydrogen bonding were expected

(23) Kricheldorf, H. R. *Org. Magn. Reson.* **1981**, *15*, 162–177.

to show differences in chemical shifts through variation in delocalization at the peptide nitrogen.

The analysis of our calculated structural shift deviations with respect to hydrogen bonding and amide proton exchange kinetics of BPTI showed no clear patterns, despite the classification of various amides into, for example, those which are buried with intrasidic hydrogen bonds and those with a high degree of solvent exposure. Other factors that might effect the nitrogen shifts, such as different  $\omega$  torsion angles, steric effects from different  $\phi$  or  $\psi$  angles, or nonneighbors, or anisotropy and ring current effects were also considered. Variations in  $\omega_{i-1}$  and  $\psi_{i-1}$  angles gave some correlations within subsets of amides. Figure 3 shows such a possible correlation for the residues in the  $\beta$  sheet region of BPTI.<sup>11,24</sup>

In summary, we have shown that a sufficiently accurate assignment of the <sup>15</sup>N chemical shifts in a small protein is practical. The correlation of this data to secondary structural features produces some qualitative relationships; however, further NMR studies on compounds with known structural data are necessary to separate the multiple factors contributing to chemical shift deviations arising from conformational effects.

**Acknowledgment.** Supported by grants from NSF, NIH, and the Keck Foundation. Bovine pancreatic trypsin inhibitor (Trasylol) was a gift from Bayer A. G.

**Supplementary Material Available:** Listing of chemical shifts and assignments (1 page). Ordering information is given on any current masthead page.

(24) The apparent dependence on  $\psi_{i-1}$  may arise from changes in the electronegativity of the oxygen of the adjacent carbonyl resulting from non-bonded interaction with the  $i$ -th amide nitrogen. Similar effects on <sup>13</sup>C shifts in cyclic carbonyl groups  $\beta$  to equatorial halogens have been observed (Metzger, P.; Casadevall, E.; Casadevall, A.; Pouet, M.-J. *Can. J. Chem.* 1980, 58, 1503-1511).

(25) Redfield, A. G.; Kunz, S.; Hurd, T. J. *Magn. Reson.* 1975, 19, 114-117.

## Total Synthesis of ( $\pm$ )-Mitomycins via Isomitomycin A

Tohru Fukuyama\* and Lihu Yang

Department of Chemistry, Rice University  
Houston, Texas 77251

Received July 28, 1987

Mitomycin C **1** is one of the most effective antitumor agents currently used for chemotherapy.<sup>1</sup> Recent studies on the mode of action have revealed a direct evidence of DNA cross-linking by **1**.<sup>2</sup> Although a number of synthetic chemists have been trying to synthesize this small, yet formidable molecule,<sup>3</sup> only one successful total synthesis has been reported to date.<sup>4</sup> While construction of the reactive quinone and aziridine rings presents serious difficulties, the major synthetic problem is how to prevent the elimination of methanol from the 9a position.<sup>5</sup> Scientists at

(1) (a) Remers, W. A. *The Chemistry of Antitumor Antibiotics*; Wiley: New York, 1979. (b) Carter, S. K.; Crooke, S. T. *Mitomycin C: Current Status and New Developments*; Academic Press: New York, 1979.

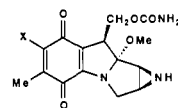
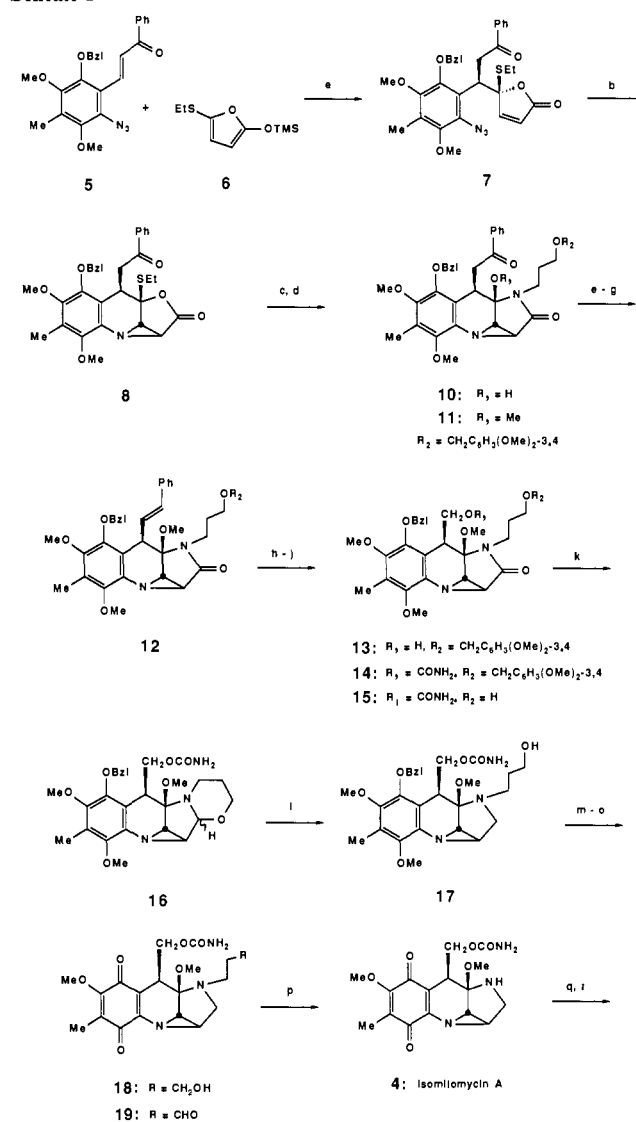
(2) Tomasz, M.; Lipman, R.; Chowdary, D.; Pawlak, J.; Verdine, G. L.; Nakanishi, K. *Science (Washington, D.C.)* 1987, 235, 1204 and references therein.

(3) For some representative approaches, see: (a) Danishefsky, S.; Berman, E. M.; Ciufolini, M.; Etheredge, S. J.; Segmuller, B. E. *J. Am. Chem. Soc.* 1985, 107, 3891. (b) Shaw, K. J.; Luly, J. R.; Rapoport, H. *J. Org. Chem.* 1985, 50, 4515. (c) Rebek, J., Jr.; Shaber, S. H.; Shue, Y.-K.; Gehret, J.-C.; Zimmerman, S. *J. Org. Chem.* 1984, 49, 5164 and references therein. (d) Franck, R. W. *Fortschr. Chem. Org. Naturst.* 1979, 38, 1.

(4) (a) Nakatsubo, F.; Fukuyama, T.; Cocuzza, A. J.; Kishi, Y. *J. Am. Chem. Soc.* 1977, 99, 8115. (b) Fukuyama, T.; Nakatsubo, F.; Cocuzza, A. J.; Kishi, Y. *Tetrahedron Lett.* 1977, 18, 4295. (c) Kishi, Y. *J. Nat. Prod.* 1979, 42, 549.

(5) For an example of facile methanol elimination, see: Danishefsky, S.; Egbertson, M. *J. Am. Chem. Soc.* 1986, 108, 4648.

## Scheme 1<sup>a</sup>



2: X = OMe Mitomycin A  
1: X = NH<sub>2</sub> Mitomycin C

<sup>a</sup> (a) SnCl<sub>4</sub> (0.1 equiv), CH<sub>2</sub>Cl<sub>2</sub>, -78 °C; 3 N HCl, THF, CH<sub>2</sub>Cl<sub>2</sub>, room temperature. (b) Toluene, 110 °C, 2 h. (c) **9** (1.6 equiv), CH<sub>2</sub>Cl<sub>2</sub>, 40 °C, 1 h. (d) MeI (5 equiv), 1 M *t*-BuOK/*t*-BuOH (1.1 equiv), THF, room temperature. (e) NaBH<sub>4</sub>, MeOH, room temperature. (f) SOCl<sub>2</sub> (2 equiv), 2,6-lutidine (10 equiv), CH<sub>2</sub>Cl<sub>2</sub>, room temperature. (g) LiBr (5 equiv), DBU (5 equiv), DMSO, 80 °C, 10 h. (h) O<sub>3</sub>, MeOH, -78 °C; NaBH<sub>4</sub>, MeOH, -78 °C to room temperature. (i) ClCO<sub>2</sub>Ph, pyridine, room temperature; NH<sub>3</sub>, MeOH, room temperature. (j) DDQ (1.5 equiv), H<sub>2</sub>O-CH<sub>2</sub>Cl<sub>2</sub> (1:20), room temperature. (k) DIBAL, THF, room temperature. (l) NaBH<sub>3</sub>CN, MeOH, THF, room temperature. (m) H<sub>2</sub> (1 atm), 10% Pd/C, EtOH, room temperature. (n) DDQ (1.5 equiv), H<sub>2</sub>O-DMSO-acetone (1:5:40), -78 °C. (o) (COCl)<sub>2</sub>, DMSO, CH<sub>2</sub>Cl<sub>2</sub>, -78 °C; Et<sub>3</sub>N. (p) pyrrolidine (5 equiv), AcOH (10 equiv), CH<sub>2</sub>Cl<sub>2</sub>, room temperature, 3 h. (q) Al(O-*i*-Pr)<sub>3</sub> (1 equiv), MeOH, room temperature, 2 days. (r) NH<sub>3</sub>, MeOH, room temperature.

Kyowa Hakkō have recently isolated and characterized two novel antitumor antibiotics, albotomycin A (**3**) and isomitomycin A (**4**), from cultures of *Streptomyces caespitosus*, a strain which